UNCLASSIFIED

AD NUMBER

AD878493

NEW LIMITATION CHANGE

TO

Approved for public release, distribution unlimited

FROM

Distribution authorized to U.S. Gov't. agencies and their contractors; Administrative/Operational Use; DEC 1970. Other requests shall be referred to Air Force Weapons Lab., Attn: LRO, Kirtland AFB, NM 87117.

AUTHORITY

Air Force Weapons Lab ltr dtd 30 Apr 1986

THIS PAGE IS UNCLASSIFIED

THIS REPORT HAS BEEN DELIMITED
AND CLEARED FOR PUBLIC RELEASE
UNDER DOD DIRECTIVE 5200.20 AND
NO RESTRICTIONS ARE IMPOSED UPON
ITS USE AND DISCLOSURE.

DISTRIBUTION STATEMENT A

APPROVED FOR PUBLIC RELEASE;
DISTRIBUTION UNLIMITED.

AD878493

AFWL-TR-70-128

AFWL-TR-
70-128

LASER BEAM PROPAGATION THROUGH JET EXHAUSTS

Keith G. Gilbert
Capt USAF

Charles B. Hogge
Capt USAF

Walter L. Visinsky
Capt USAF

TECHNICAL REPORT NO. AFWL-TR-70-128

December 1970

AIR FORCE WEAPONS LABORATORY
Air Force Systems Command
Kirtland Air Force Base
New Mexico

AD No.
DDC FILE COPY

DDC
RECEIVED
JAN 14 1971
B

This document is subject to special export controls and each transmittal to foreign governments or foreign nationals may be made only with prior approval of AFWL (LRO), Kirtland AFB, NM, 87117.

46

AFWL-TR-70-128

AIR FORCE WEAPONS LABORATORY
Air Force Systems Command
Kirtland Air Force Base
New Mexico 87117

When U. S. Government drawings, specifications, or other data are used for any purpose other than a definitely related Government procurement operation, the Government thereby incurs no responsibility nor any obligation whatsoever, and the fact that the Government may have formulated, furnished, or in any way supplied the said drawings, specifications, or other data, is not to be regarded by implication or otherwise, as in any manner licensing the holder or any other person or corporation, or conveying any rights or permission to manufacture, use, or sell any patented invention that may in any way be related thereto.

This report is made available for study with the understanding that proprietary interests in and relating thereto will not be impaired. In case of apparent conflict or any other questions between the Government's rights and those of others, notify the Judge Advocate, Air Force Systems Command, Andrews Air Force Base, Washington, DC 20331.

DO NOT RETURN THIS COPY. RETAIN OR DESTROY.

WHITE SECTION
BUFF SECTION
DISTRIBUTION/AVAILABILITY CODES
DIST. AVAIL. and/or SPECIAL
2

AFWL-TR-70-128

LASER BEAM PROPAGATION THROUGH JET EXHAUSTS

Keith G. Gilbert, Capt, USAF

Charles B. Hogge, Capt, USAF

Walter L. Visinsky, Capt, USAF

TECHNICAL REPORT NO. AFWL-TR-70-128

This document is subject to special export controls and each transmittal to foreign governments or foreign nationals may be made only with prior approval of AFWL (LRO), Kirtland AFB, NM 87117. Distribution is limited because of the technology discussed in the report.

FOREWORD

This research was performed under Program Element 63602F, Project 644A, Task 2.

Inclusive dates of research were January 1970 and April 1970. The report was submitted 23 September 1970 by the Air Force Weapons Laboratory Project Officers, Captain Keith G. Gilbert (LRE), Captain Charles B. Hogge (LRO), and Captain Walter L. Visinsky (LRO).

Information in this report is embargoed under the Department of State ITIARs. This report may be released to foreign governments by departments or agencies of the US Government subject to approval of AFWL (LRO).

We wish to thank Capt Bill Helmich, SSgt Bob Brumley, SSgt Mike Gullo, and A1C Jim Korka for their assistance in these experiments.

This technical report has been reviewed and is approved.

KEITH G. GILBERT
Captain, USAF
Project Officer

CHARLES B. HOGGE
Captain, USAF
Project Officer

WALTER L. VISINSKY
Captain, USAF
Project Officer

DONALD L. LAMBERSON
Colonel, USAF
Chief, Laser Division

ABSTRACT

(Distribution Limitation Statement No. 2)

CO_2 (10.6 micron) and He-Ne (6328Å) laser beams were passed through the highly turbulent region in the exhaust of a jet engine (J-57 with afterburner). Experimental information was obtained on the absorption, scattering and turbulence effects of the jet exhaust on both laser beams for various propagation paths. Estimates of a structure constant that would characterize the turbulence in the exhaust are made from the beam spread of focused and collimated beams. The structure constant obtained in this manner is then compared with the structure constant determined from scintillation measurements on the CO_2 beam and with the results of hot-wire anemometer readings in the exhaust. The various methods yield results for the structure constant that are in good agreement (typically a structure constant of the order of $3 \times 10^{-5} m^{-1/3}$).

CONTENTS

Section		Page
I	INTRODUCTION	1
II	THEORY	2
	Scintillation	2
	Beam Spread	[illegible]
	Anemometers	5
III	EXPERIMENTAL RESULTS	6
	Anemometer Measurements	6
	Scintillation Measurements for the 10.6μ Beam	7
	Beam Spread Measurements	10
	Absorption Measurements	17
IV	DISCUSSION OF RESULTS	22
	Assumptions	22
	Absorption	23
	Scintillation	23
	Beam Spread	24
V	FUTURE STUDIES	25
	APPENDIXES	
	I Beam Spreading of CO_2	27
	II Night Experiment with He-Ne	30
	REFERENCES	35

ILLUSTRATIONS

Figure		Page
1	Location of Equipment and Propagation Paths Used in Experiment	8
2	Beam Spread for Focused He-Ne Beam on 11 February 1970	11
3	Beam Spread for Various Engine Power Settings--Focused He-Ne Beam 12 February 1970	12
4	Beam Spread for Various Engine Power Settings--Collimated He-Ne Beam, 17 February 1970	13
5	Beam Spread for Various Engine Power Settings--Collimated He-Ne Beam, 18 February 1970	14
6	Beam Spread for Various Engine Power Settings--Focused He-Ne Beam, 18 February 1970	15
7	Beam Spread for Focused He-Ne Beam Using J-97 Jet Exhaust on 31 March 1970	16
8	Normalized Power versus Aperture Diameter for Collimated CO_2 Beam on 11 and 12 February 1970	28
9	Beam Spread for Focused CO_2 Beam on 17 February 1970	29
10	Collimated Beam Before Jet Engine was Started. Note that Whisper Modes are Visible Outside the Main Beam	31
11	As the Jet Engine is Started, the Beam Immediately Begins to Expand. The Expansion Shown here is not Radially Symmetrical.	31
12	Expanse of the Collimated Beam with the Jet Engine at Idle Power	32
13	Expanded Beams with the Jet Engine in Afterburner. The Dark Spots Throughout the Expanded Beam were Observed to Move Horizontally Left to Right Through the Beam. The Laser was Located on the Left Side of the Exhaust with the Receiving Screen on the Right.	33
14	Sputtering of the Beam After Jet Engine Shut-Down. Note the Vertical Structure of the Sputtering Caused by the Rising Hot Gases Immediately Behind the Jet Engine	34
15	Another Form of Sputtering Observed After Engine Shut-Down--This One with What Seems to be a Ring Shape.	34

TABLES

Table		Page
I	ΔT_{RMS} Readings from Anemometer Probes	6
II	Meteorological Conditions for 15 and 16 January 1970	7
III	Jet Engine Power Settings and Characteristics	9
IV	Variance and Calculated Structure Constant for CO_2 Scintillation Measurements	9
V	Beam Spread and Corresponding Structure Constant for He-Ne Propagation Through Jet Exhaust Using $\Omega = \pi\omega_o^2/\lambda z$	18
VI	Beam Spread and Corresponding Structure Constant for He-Ne Propagation Through Jet Exhaust Using Ω_f for Focused Beams and Ω for Collimated Beams	19
VII	Beam Spread and Corresponding Structure Constant for He-Ne Propagation Through Jet Exhaust Using Ω_f for Both Collimated and Focused Beams	20

ABBREVIATIONS AND SYMBOLS

A	Amplitude
C_ℓ	Log amplitude variance
C_ℓ^s	Spherical wave variance
C_n	Structure constant
CO_2	Carbon dioxide
D	Diameter of transmitting aperture
G	Davis' factor for aperture averaging
He-Ne	Helium-Neon
P	Power; ambient pressure
ΔT_{RMS}	Root-mean-square temperature fluctuations
V_n	Velocity of wind normal to laser beam
d	Diameter of receiver aperture
f_{max}	Maximum frequency of scintillations
k	Wave number
$\langle \ell \rangle$	Mean of the log amplitude variance
Z	Range
Ω	Dimensionless parameter = $\pi\omega_o^2/\lambda z$
λ	Wavelength
σ_a	Variance of amplitude fluctuations
σ_p	Variance of power fluctuations
ω	Radius of beam at receiver with no turbulence
ω_o	Radius of beam at transmitter
ω_t	Radius of beam at receiver with turbulence

SECTION I

INTRODUCTION

To date, most experimental propagation work has been performed over long ranges (200 m to 20 km). The primary use of these tests has been to verify existing propagation theories. In our work here we attempt to use existing theory to quantitatively probe the exhaust of a jet engine. Consequently, we try to characterize the turbulence in the exhaust by the well-known "structure constant C_n" occurring in most propagation theories (Ref. 1).

However, because we do not know of any existing experimental verification of some of the theories used here, we have attempted to correlate the experimental results for C_n obtained using these propagation theories with measurements of C_n using pairs of hot wire anemometers in the jet exhaust. While this was not the primary intent of our work, we felt this correlation was necessary in order to establish a confidence level in the optical measurement techniques.

We used two radiation sources for our work, a He-Ne laser operating at 0.63 micron with an output power between 10 and 20 milliwatts and a CO_2 laser operating at 10.6 microns with an output between 20 and 40 watts. The He-Ne laser was operated in the TEM_{oo} mode while the CO_2 laser was highly multimoded. As a result of this and the inherent operating instabilities of the CO_2 laser, most usable data were obtained with the 0.63 micron beam. However, because the gas constituents in the jet exhaust characteristically absorb more strongly at infrared wavelengths, we decided to further use the 10.6-micron beam to make estimates of extinction coefficient for this wavelength. The multimode nature of the beam does not appreciably degrade the measurement of this parameter.

A J-57 jet engine was used for most experiments. The engine was operated in a variety of power settings ranging from idle (60 percent maximum power) to afterburner. We tried various path directions and distances through the exhaust.

Therefore, aside from the absorption measurement at 10.6 microns, we were primarily interested in measuring beam spread and beam scintillation. These quantities can be readily related to existing theories from which the quantity of interest, C_n, can be calculated.

SECTION II

THEORY

1. SCINTILLATION

Scintillation as used in propagation theory is the fluctuation of the received intensity both in space and time. While the temporal fluctuations are the easiest to measure, and therefore their equivalence to spatial fluctuation often argued, the latter is usually the one most often theoretically treated. Fortunately, under the assumption of "frozen in" turbulence, the statistical nature of both spatial and temporal fluctuation seems to be the same. Tatarski (Ref. 1) shows in his work that the variance of the spatial scintillation of a plane wave assuming a Kolmogorov spectrum of turbulence is given by

$$\overline{\sigma_a^2} = .31\ C_n^2\ k^{7/6}\ z^{11/6}$$

where

$\overline{\sigma_a^2}$ = log amplitude variance = $\overline{\left[\log\left(A/A_o\right)\right]^2}$

A = the field variable

C_n = structure constant associated with refractive index variations

k = wave number = $2\pi/\lambda$

z = path length of the propagation

Since the amplitude fluctuations may be related to the intensity fluctuations

$$4\left[\log\left(A/A_o\right)\right]^2 = \left[\log\left(I/I_o\right)\right]^2$$

we then have

$$\overline{\sigma_I^2} = 1.23\ C_n^2\ k^{7/6}\ z^{11/6} \tag{1}$$

where

$\overline{\sigma_I^2}$ = log intensity variance

If we wish to consider the power fluctuations in the measurement plane, we must include the aperture averaging effects as described by Davis (Ref. 2). This leads to

$$\overline{\sigma_P^2} = \overline{\sigma_I^2}\ G\left[D/(\lambda z)^{1/2}\right]\ G\left[d/(\lambda z)^{1/2}\right]$$

where

$\overline{\sigma_P^2}$ = power variance

D = transmitting aperture diameter

d = receiving aperture diameter

Davis lists values of G for various values of the parameters (Ref. 2).

Let us next define

$$\overline{X_P^2} = \overline{\left[P^2 - \overline{P}^2\right]/\overline{P}^2}$$

where $\overline{P}$ = average power without turbulence. Experimental evidence (Ref. 3) supports the hypothesis that the log amplitude (and therefore the log intensity) is normally distributed. Furthermore, first order Rytov theory predicts the mean of the log amplitude is zero. Under this assumption, one can show that the variance of the intensity (power) is related to the log intensity (power) by

$$\overline{\sigma_P^2} = \log\left(1 + \overline{X_P^2}\right)$$

By monitoring the fluctuations in received power, we can then calculate the variance of the log intensity and determine the corresponding structure constant which this variance represents.

2. BEAM SPREAD

In the propagation of beam waves, the small angle scattering caused by turbulent eddies not only produces the scintillation effect already discussed for plane waves, but it also produces beam spreading. This is equally true for collimated and focused beams. The theoretical problem of beam wave propagation has been treated by several people. For our work we have used most extensively the results of Fried and Seidman (Ref. 3) and Gebhardt (Ref. 4).

The assumptions are that

(1) energy is conserved in going from the transmitter to the receiver plane,

(2) the resulting average intensity profile is still gaussian in shape, and

(3) the log amplitude is normally distributed with mean equal to $\langle \ell(R) \rangle$ and variance equal to $C_\ell(R)$, where R is the radius vector referenced to the optical axis of the beam.

Gebhardt has shown, using the above assumptions, that the ratio of the average radius (spot size) of the beam with turbulence (ω_t) to the theoretical radius in the absence of turbulence (ω) is given by*

$$\left(\omega_t/\omega\right) = \exp\left[-\left(\langle \ell(0) \rangle + C_\ell(0)\right)\right] \tag{2}$$

If $C_\ell^s(0)$ is the variance of the log amplitude for a spherical wave, given by (Ref. 1)

$$C_\ell^s(0) = 0.124\ C_n^2\ k^{7/6}\ z^{11/6} \tag{3}$$

then one can show that the ratios $\left[\langle \ell \rangle / C_\ell^s\right]$ and $\left[C_\ell / C_\ell^s\right]$ depend only on a dimensionless parameter

$$\Omega = \left(\pi \omega_o^2 / \lambda z\right) \tag{4}$$

where ω_o is the radius of the transmitter. Gebhardt has tabulated the values of $\left[\langle \ell \rangle / C_\ell^s\right]$ as a function of Ω for the case of a focused and collimated beam

---

*Gebhardt has shown that retaining second order terms in the Rytov solution produces a non-zero average value for the log amplitude which is numerically of the order of $C_\ell(0)$.

while Fried and Seidman have tabulated $\left[C_\ell/C_\ell^s\right]$ for the same cases. In terms of the normalized ratios, equation (2) can be rewritten as

$$\left(\omega_t/\omega\right) = \exp\left\{- C_\ell^s(0)\left[\left[\langle\ell\rangle/C^s(0)\right] + \left[C_\ell(0)/C_\ell^s(0)\right]\right]\right\} \tag{5}$$

Clearly, by determining the spread of the focused and collimated beams in the receiver plane, one can determine an effective structure constant, C_n.

3. ANEMOMETERS

As indicated earlier, we attempted to correlate the measurements of C_n obtained using the "optical techniques" just discussed with a measurement of the structure constant using hot wire anemometers calibrated as resistance thermometers. The basic operation of these devices has been discussed extensively in literature (Ref. 5) and therefore we will only present here the relationship between the measured temperature fluctuations variance T_{RMS} and C_n.

$$C_n = (77.6/T^2)\ P\ \Delta\ T_{RMS} \times 10^{-6}\left(R^{-1/3}\right) \tag{6}$$

where

P = ambient pressure in millibars

T = ambient temperature in °K

ΔT_{RMS} = root-mean-square temperature fluctuations in °K

R = the separation distance between the probes

SECTION III

EXPERIMENTAL RESULTS

1. ANEMOMETER MEASUREMENTS

Hot wire anemometers were used on 15 and 16 January 1970 to record ΔT_{RMS} in the engine exhaust (Ref. 6). The probes were placed in the following positions:

15 January--The two 0.00015-inch diameter platinum wire probes were separated in the vertical by a distance of 14 cm. The plane of the probes was normal to the axis of the jet exhaust and placed about three feet back from the nozzle. The probes were 18 inches below and 4-1/2 feet to the side of the center line of the exhaust.

16 January--The same equipment was used as on 15 January with the probes moved 13 feet away from the nozzle and placed more directly into the exhaust (6 inches below and 3 feet to the side of the center line). The probes were separated in the vertical by a distance of 4.5 cm.

The ΔT_{RMS} readings were taken directly from a 2400A Hewlett Packard true root-mean-square meter. The 2-second RMS readings are given in table I.

Table I

ΔT_{RMS} READINGS FROM ANEMOMETER PROBES

Date	Engine Power (%)	Meter Scale (mv)	Voltage RMS Reading	ΔT_{RMS} (°F)
15 Jan 70	75	1	Negligible	
15 Jan 70	90	1	.3	.11
15 Jan 70	100	No readings due to vibration		
16 Jan 70	75	10	.3	.66
16 Jan 70	90	10	.5	1.1

The meteorological conditions for both days are shown in table II.

Table II

METEOROLOGICAL CONDITIONS FOR 15 AND 16 JANUARY 1970

Item	15 Jan	16 Jan
Pressure	830.3MB	836.8MB
Temperature	43°F	50°F
Water Vapor	4400PPM	3300PPM
Weather	Broken clouds at 4000 feet, visibility 40 miles	Clear

Neglecting the water vapor contribution, we can solve for C_n using equation (6). If we use the atmospheric ambient temperature, the 0.11° and 1.1° F readings at the 90 percent power setting correspond to C_n's of 4.22×10^{-7} and $4.16 \times 10^{-6} m^{-1/3}$, respectively. If instead we use the temperature at the probes (as measured by a thermocouple attached to one of the probes), we obtain 3.7×10^{-8} and 1.6×10^{-6} for C_n, respectively. Recalling that heavy atmospheric turbulence is defined as a C_n of $5 \times 10^{-7} m^{-1/3}$ (Ref. 2), we note that the readings of 16 January 1970 are approximately two to ten times greater than this value.

Note that on both days the probes were placed to one side of the jet exhaust centerline. Attempts to measure the heavy turbulence in this region of the exhaust failed when the filaments were repeatedly blown off their holders.

2. SCINTILLATION MEASUREMENTS FOR THE 10.6μ BEAM

The scintillation measurements were made on 16 January 1970 using the CO_2 laser and the diagonal path indicated in figure 1. A 4-mm pinhole was centered on a 4-inch collecting mirror in the receiving plane and the power fluctuations through the pinhole were measured by a 201 calorimeter and recorded on a visicorder. The jet engine was run at the power settings indicated in table III.

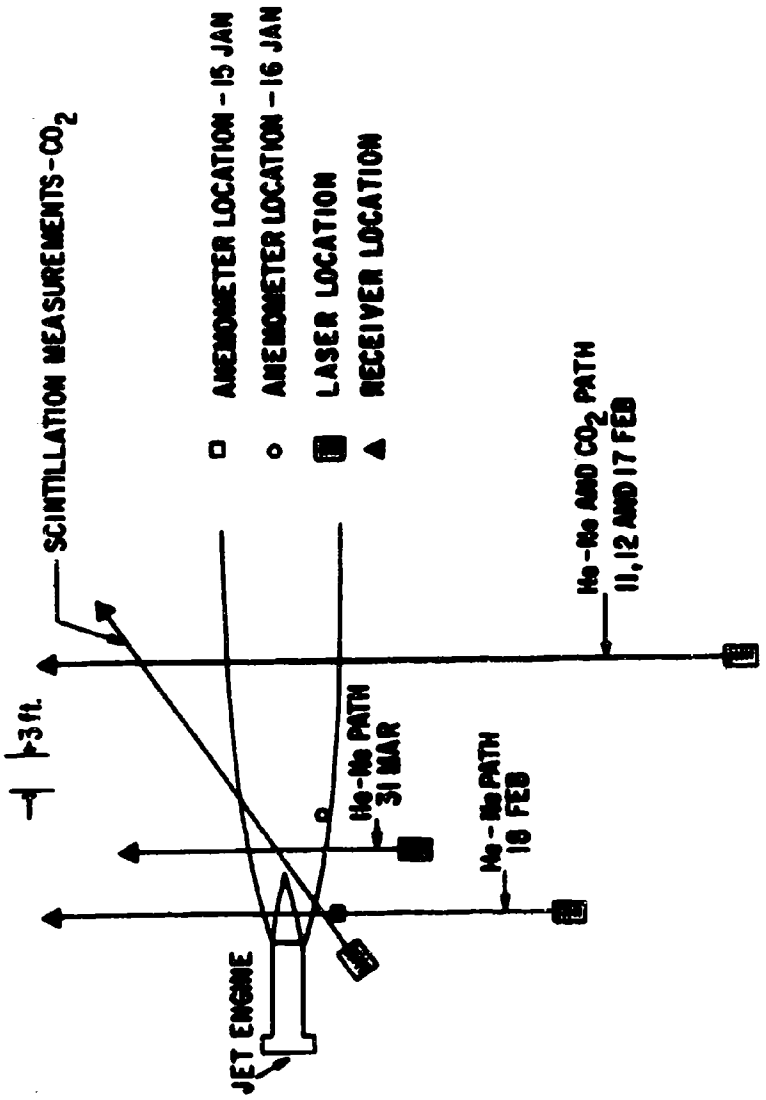

Figure 1. Location of Equipment and Propagation Paths Used in Experiment

Table III

JET ENGINE POWER SETTINGS AND CHARACTERISTICS

Engine Power (%)	Duration (min)	Exhaust Temp (°F)	Fuel Flow (lbs/hr)
idle	3	560	990
75	3	630	1,775
90	3	1010	6,000
100	3	1125	7,600
afterburner	1	1140	26,500

Measurable scintillation was observed only while the engine was at idle. The maximum frequency of scintillation increases like $f_{max} = V_n/(\lambda z)^{1/2}$, where V_n is the effective exhaust velocity normal to the laser beam, and as a result at higher exhaust velocities, the calorimeter used to detect the 10.6μ radiation could not respond to the more rapid fluctuations.

The structure constant of the turbulence in the jet exhaust at idle was evaluated using the formulation in Section II.1. Three different times during the engine run, the structure constant was evaluated. The results are given in table IV.

Table IV

VARIANCE AND CALCULATED STRUCTURE CONSTANT FOR CO_2 SCINTILLATION MEASUREMENTS

Variance $\left(\sigma_p^2\right)$	C_n (Calculated)
9.4×10^{-3}	1.46×10^{-5}
4.7×10^{-3}	1.04×10^{-5}
1.51×10^{-2}	1.81×10^{-5}

We can see from these calculations that the turbulence, as evidenced by the structure constant, in the jet exhaust changes with time (intuitively it must since a jet engine exhaust is not at constant temperature or velocity but exhibits fluctuations about some mean which itself may change with time). However, the results in table IV are relatively constant for this propagation path.

3. BEAM SPREAD MEASUREMENTS

The effective spread of both collimated and focused beams at the receiver plane was determined by using a variable receiving aperture iris and a power meter. By plotting average power versus receiving aperture radius, one is able to readily determine the effective $1/e^2$ points (spot size or radius) of both the perturbed and unperturbed beams. For these experiments, the jet engine was operated at the power settings indicated in table I. Figures 2 through 7 show the plots of beam spread for the various cases considered as a function of normalized received power versus receiver aperture diameter.

Once the effective radii for a particular perturbed and unperturbed beam are determined, we can use the formalism developed in Section II.2 to determine an effective, "average"* structure constant for the particular path considered. As we indicated earlier, only the measurements obtained using the focused and collimated 0.63μ beam were considered meaningful. The collimated 10.6μ beam had such a small beam spread that accurate measurements were difficult under the experimental conditions at hand. The focused 10.6μ beam was of such poor quality that it was decided that useful quantitative comparison with theoretical predictions would be impossible. However, we do include in Appendix I the experimental results for a collimated and a focused 10.6μ beam.

Analysis of the data may be performed in at least three ways. One method is as follows: (1) measure ω_o, and ω_t in the receiving plane; (2) calculate $\Omega = \pi\omega_o^2/\lambda z$ and the beam spread ratios ω_{tf}/ω_f and ω_{tc}/ω_c where $\omega_f = \lambda z/\pi\omega_o$ is the diffraction limited focal spot size (Ref. 3), $\omega_c = \omega_o$ is the collimated beam spot size, and where ω_{tf} and ω_{tc} are the average spot sizes of the focused and collimated beams, respectively, in turbulence; (3) obtain $\left[C_\ell(0)/C_\ell^s(0)\right]$ and

*In the truest sense of the word, we do not obtain an average C_n over the path of propagation. The theoretical formulation indicates that the incorporation of the spatial dependence of C_n can be quite complicated (see Ishimaru, Ref. 7). However, for a "first cut" measure of the turbulence, we have assumed that the averaging which does occur closely approximates a true averaging operation.

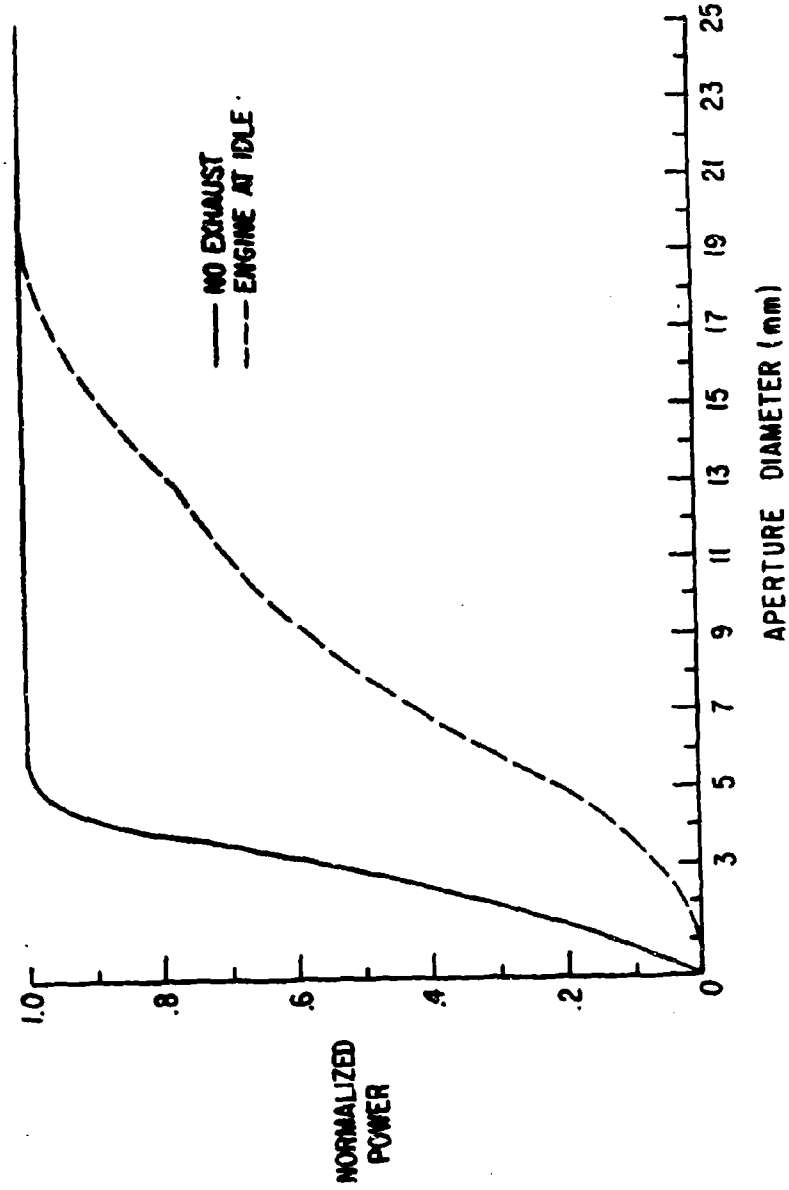

Figure 2. Beam Spread for Focused He-Ne Beam on 11 February 1970

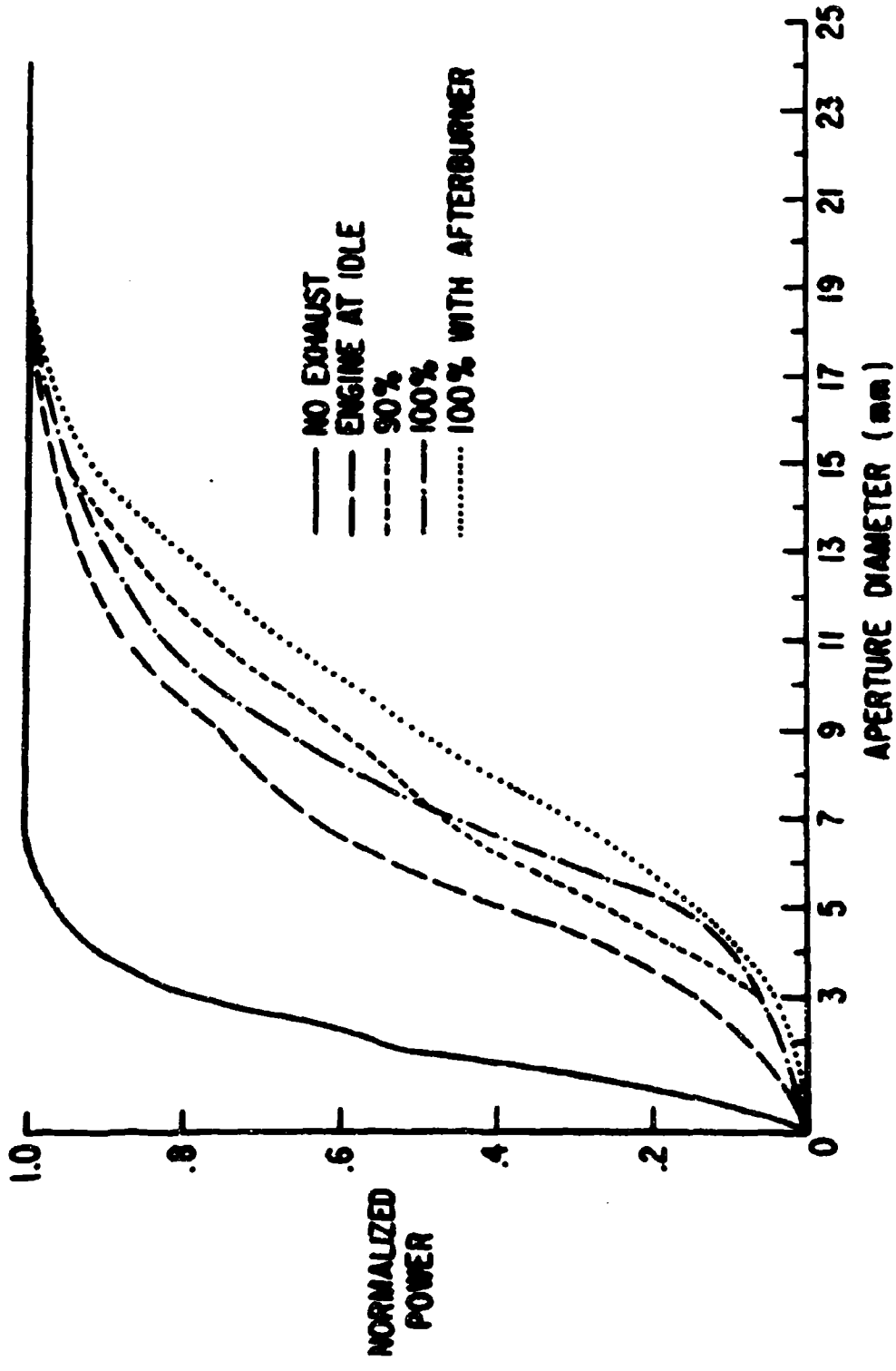

Figure 3. Beam Spread for Various Engine Power Settings
Focused He-Ne Beam 12 February 1970

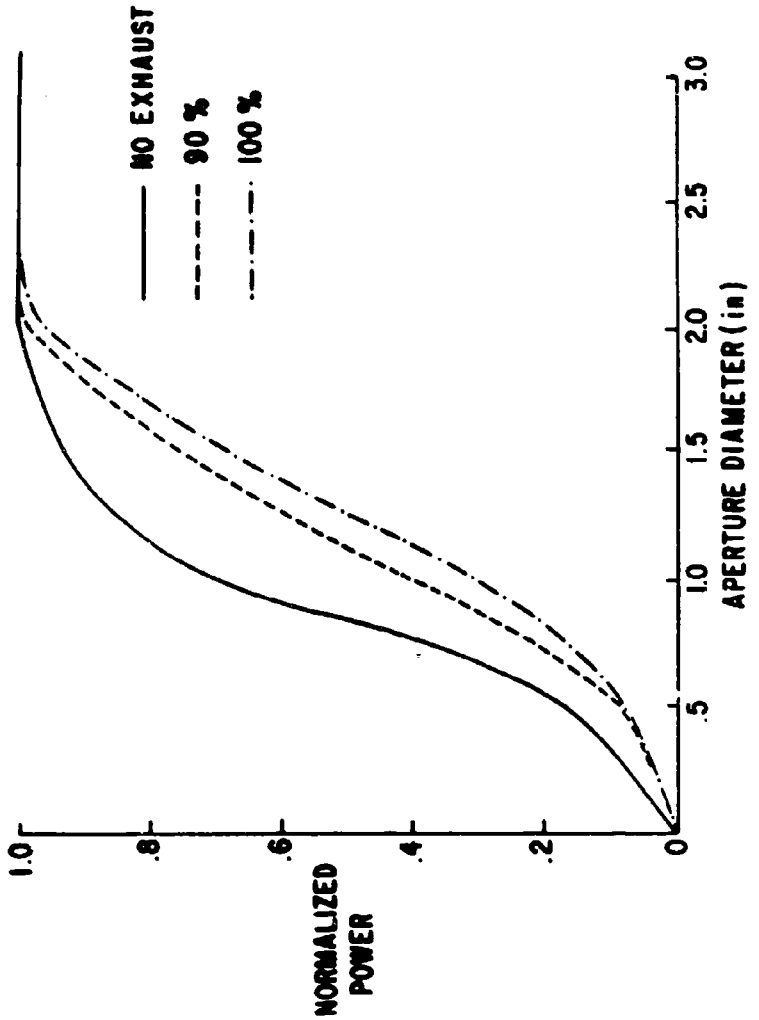

Figure 4. Beam Spread for Various Engine Power Settings
Collimated He-Ne Beam, 17 February 1970

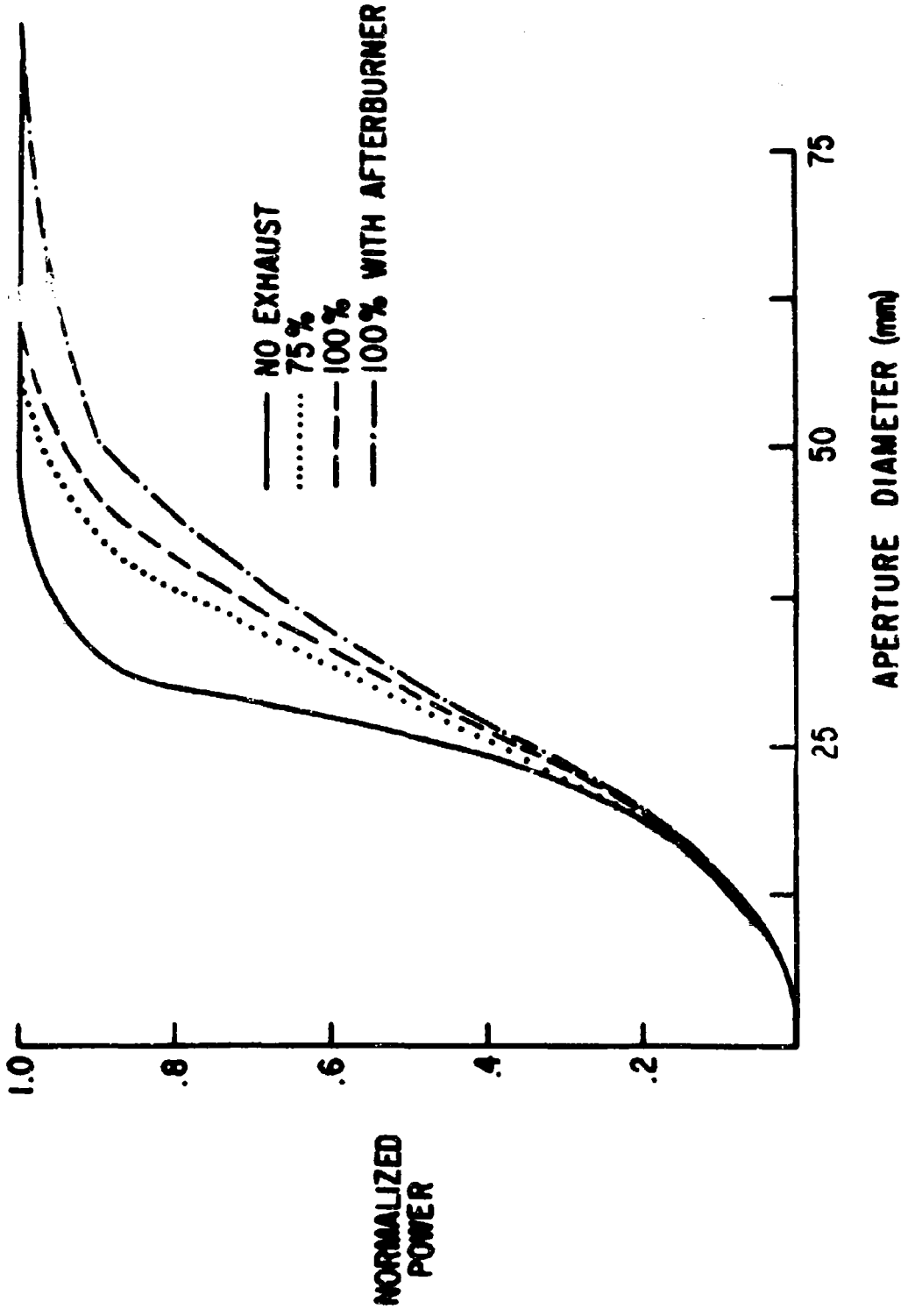

Figure 5. Beam Spread for Various Engine Power Settings
Collimated He-Ne Beam, 18 February 1970

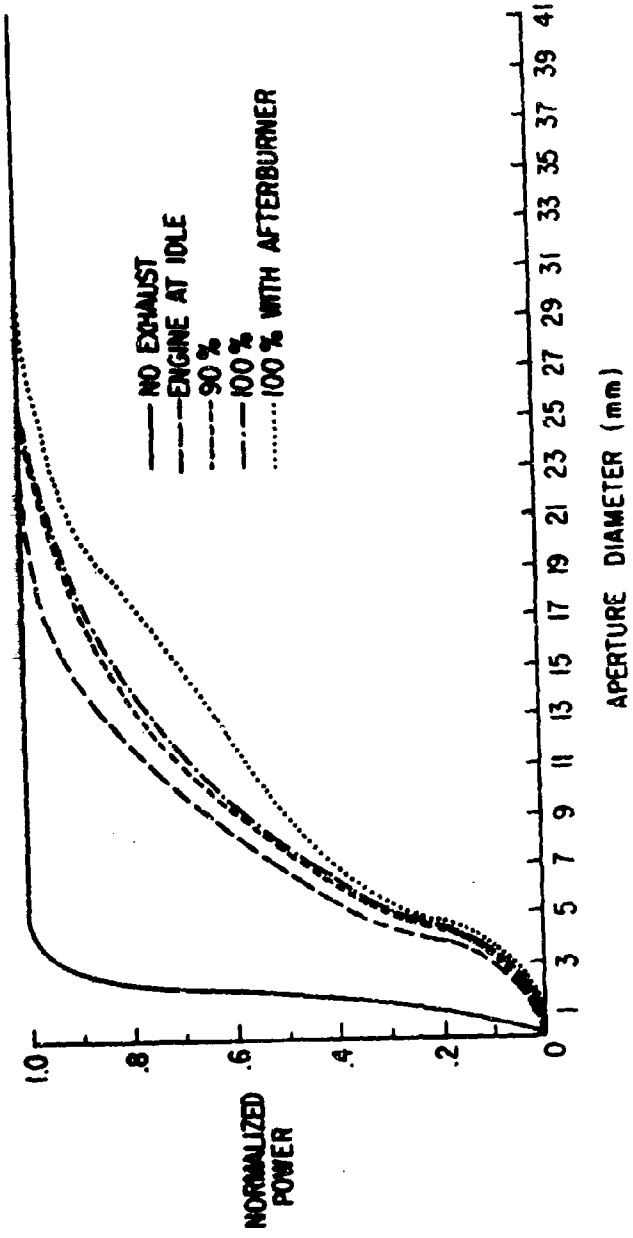

Figure 6. Beam Spread for Various Engine Power Settings
Focused He-Ne Beam, 18 February 1970

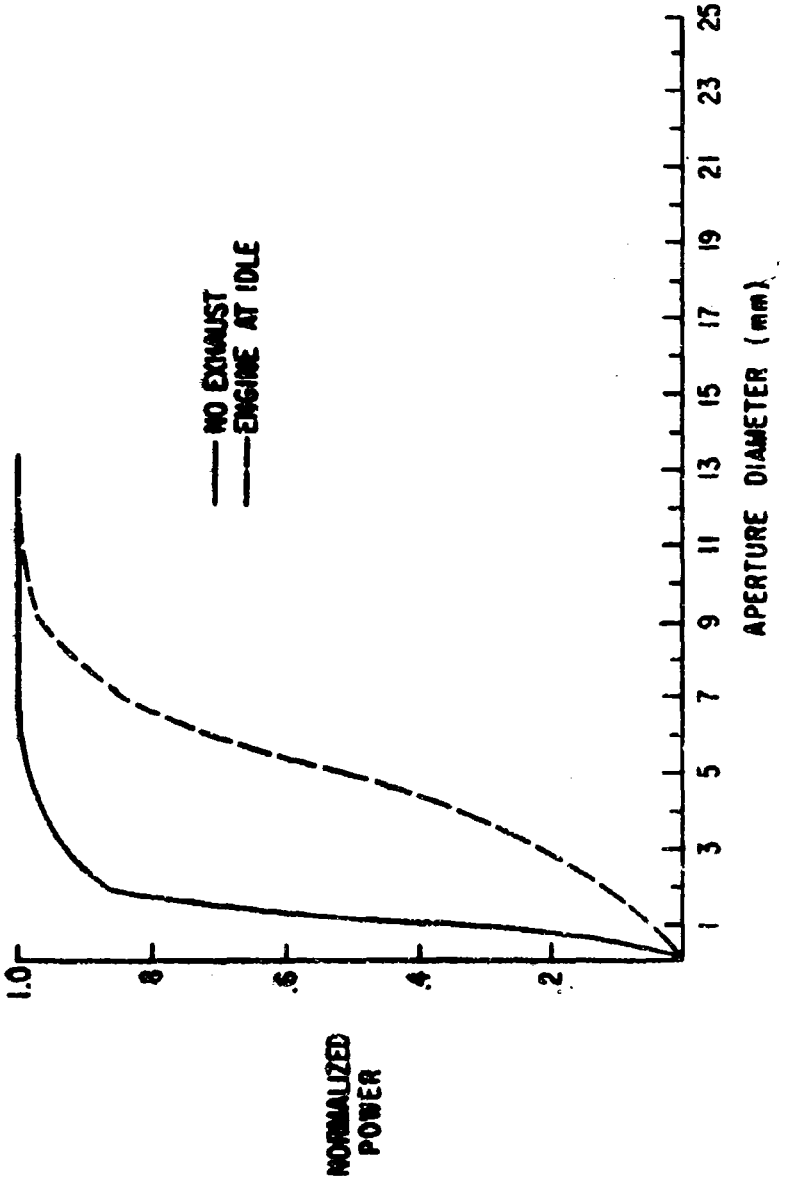

Figure 7. Beam Spread for Focused He-Ne Beam Using J-97 Jet Exhaust on 31 March 1970

and collimated beams, respectively, in turbulence; (3) obtain $\left[C_\ell(0)/C_\ell^s(0)\right]$ and $\left[\langle\ell\rangle/C_\ell^s(0)\right]$ from the published tables; and then (4) solve for C_n. The results for C_n using this method are presented in table V.

For the special case of a focused beam, one can show that Ω is also correctly given for a diffraction limited optical system by ω_o/ω_f. In practice, the measured focal spot size ω_{fm} is seldom equal to the diffraction limited spot size ω_f. A better measure of the beam spread may therefore be given by $\omega_o/\omega_{fm} = \Omega_f$ rather than by $\Omega = \omega_o/\omega_f = \pi\omega_o^2/\lambda z$. Thus, a second method of data analysis may be as follows: (1) measure ω_o, ω_{fm}, and ω_{tf} in the receiver plane; (2) calculate $\Omega_f = \omega_o/\omega_{fm}$ and the beam spread ratio ω_{tf}/ω_{fm}; (3) obtain $\left[C_\ell(0)/C_\ell^s(0)\right]$ and $\left[\langle\ell\rangle/C_\ell^s(0)\right]$ using Ω_f; and (4) solve for C_n. This method is specifically used for focused beam propagation. For the collimated beam, one can only measure ω_c at the receiver plane. While the optical system used was not diffraction limited, it is believed that, within the measurement accuracy, ω_c gives a very good estimate of ω_o for these short propagation paths. Hence, it is believed that $\Omega_c = \pi\omega_c^2/\lambda z$ would be more appropriate for determining C_n when a collimated beam is used. Note, however, this implies that, for a non-diffraction limited system, $\Omega_f \neq \Omega_c$. Applying this procedure to the focused beams, the values yielded for C_n are given in table VI. The results for the collimated beams are clearly the same as those obtained using the previous procedures.

Yet a third method for analyzing the data is suggested by the fact that $\Omega_c \neq \Omega_f$. Thus, one might do the following: (1) repeat the steps of method 2; and then (2) apply the values of Ω_f obtained by $\left(\omega_o/\omega_{fm}\right)$ to the collimated beam analysis. These results are given in table VII. In this table, the results for the focused beam propagation are clearly the same as given in table VI and therefore are not presented here. Note that because ω_{fm} differed for two successive runs with the same path (16.8 m), different values of Ω_f are used.

4. ABSORPTION MEASUREMENTS

Extinction coefficients for the CO_2 10.6μ laser were measured in the J-57 engine exhaust along two paths. A slant path traversed 5 meters of turbulent medium while the perpendicular path included 3 meters of exhaust environment (figure 1). The CO_2 laser nominally produced 50 watts of multimode power for these experiments. Source power was continuously monitored by means of a

Table V

BEAM SPREAD AND CORRESPONDING STRUCTURE CONSTANT FOR He-Ne PROPAGATION THROUGH JET EXHAUST USING $\Omega = \pi\omega_o^2/\lambda z$

Date	$L^{(m)}$	Ω	$\omega_f x10^3 m$	$\omega_o = \omega_c (x10^3 m)$	% Engine Power	$\omega_{tc} x10^3 m$	$\omega_{tf} x10^3 m$	$C_n x10^5 m^{-1/3}$
				Focused Beam				
11 Feb	16.8	77.9	.21	16.2	Idle	NA	7.35	2.31
12 Feb	16.8	77.9	.21	16.2	Idle	NA	5.2	2.20
					90		5.8	2.23
					100		6.3	2.26
					100/AB*		6.8	2.29
18 Feb	12.4	96.6	.16	15.5	Idle		6.6	3.12
					90		7.9	3.19
					100		8.1	3.20
					100/AB		9.6	
				Collimated Beam				
17 Feb	16.8	77.9	NA	16.2	90	20.2	NA	2.68
					100	23.2	NA	3.43
18 Feb	12.4	96.6	NA	15.5	75	20.6	NA	3.96
					100	21.6	NA	4.32
					100/AB	23.9	NA	4.94

*Afterburner

Table VI

BEAM SPREAD AND CORRESPONDING STRUCTURE CONSTANT FOR He-Ne PROPAGATION THROUGH JET EXHAUST USING Ω_f FOR FOCUSED BEAMS AND Ω FOR COLLIMATED BEAMS

Date	$L^{(m)}$	Ω_f	$\omega_{fm} x10^3 m$	$\omega_o = \omega_c (x10^3 m)$	% Engine Power	$\omega_{tc} x10^3 m$	$\omega_{tf} x10^3 m$	$C_n x10^5 m^{-1/3}$
				Focused Beams*				
11 Feb	16.8	8.1	2.0	16.2	Idle	NA	7.4	1.51
12 Feb	16.8	9.5	1.7	16.2	Idle	NA	5.2	1.39
					90		5.8	1.45
					100		6.3	1.50
					100/AB**		6.8	1.55
18 Feb	12.4	11.9	1.3	15.5	I	NA	6.6	2.19
					90		7.9	2.30
					100		8.1	2.32
					100/AB		9.6	2.43

*For Collimated Beams see table V.
**Afterburner

Table VII

BEAM SPREAD AND CORRESPONDING STRUCTURE CONSTANT FOR He-Ne PROPAGATION THROUGH JET EXHAUST USING Ω_f FOR BOTH COLLIMATED AND FOCUSED BEAMS

Date	$L^{(m)}$	Ω_f	$\omega_{fm} x10^3 m$	$\omega_o = \omega_c (x10^3 m)$	% Engine Power	$\omega_{tc} x10^3 m$	$\omega_{tf} x10^3 m$	$C_n x10^5 m^{-1/3}$
				Collimated Beams*				
19 Feb	16.8	8.1	2.0	16.2	90	20.2	NA	1.19
					100	23.2	NA	1.52
17 Feb	16.8	9.5	1.7	16.2	90	20.2	NA	1.23
					100	23.2	NA	1.57
18 Feb	12.4	11.9	1.3	15.5	75	20.6	NA	1.93
					100	21.6		2.11
					100/AB**	23.9		2.41

*For Focused Beams see table VI
**Afterburner

potassium chloride (KCl) beam splitter and standard thermopile. That part of the laser beam crossing the exhaust region was gathered by a 4-inch mirror located 9 meters from the exhaust and focused on a thermopile. The CO_2 beam was approximately 3 inches in diameter at the receiving mirror.

Absorption measurements on the slant path were made at engine power settings of 100 percent and afterburner. Two independent measurements showed beam absorption at these power settings of 7 percent $\pm$ 3 percent and 22 percent $\pm$ 4 percent, respectively (errors shown are RMS errors). Corresponding extinction coefficients are 0.0145 m^{-1} and 0.0497 m^{-1}. Beam absorption at lower power settings was found to be negligible. Along the shorter (3 meter) path only absorption with engine in afterburner configuration was measurable. Results of several measurements yielded an absorption of 15 percent $\pm$ 1.5 percent with a corresponding extinction of 0.0542 m^{-1}.

SECTION IV

DISCUSSION OF RESULTS

1. ASSUMPTIONS

In performing these calculations several assumptions which are of importance to the fundamental validity of the conclusions have been made and should be indicated here. First, it was assumed that C_n was essentially constant throughout a plane perpendicular to the exhaust. This clearly is not true, and while its full implications on the results presented here are not completely understood, it is felt that the measurements give reasonable estimates of the effective turbulence in the exhaust. However, this assumption probably introduces the greatest uncertainty into the results of any of the approximations made.

Secondly, it was assumed that the propagation path began at the edge of the jet exhaust. Therefore, any atmospherically induced turbulence up to this point is neglected. Upon leaving the exhaust, it was then assumed that a simple geometric projection accurately modeled the propagation to the detector plane, again neglecting atmospherically induced turbulence. Actually, these assumptions are probably good in view of the fact that the actual distance between the transmitter and the receiver was only slightly larger than the effective jet exhaust diameter for most cases.

Thirdly, it was assumed that for the 0.63μ beam, atomic and molecular absorption were small. The theoretical beam spreading formulation assumes this, and the exact implications of not satisfying this are not really understood. However, it is fortunate that the 0.63μ beam was only slightly attenuated by absorption in passing through the jet exhaust.

Finally, in the theoretical developments of Fried and Seidman and Gebhardt, it is assumed that a Kolmogorov spectrum (Ref. 1) of turbulence exists. Because the numerical results of the above authors are used for the evaluation of $\left[\langle \ell(0)\rangle / C_\ell^s(0)\right]$ and $\left[C_\ell(0) / C_\ell^s(0)\right]$, it is clear that the same assumption is made here for the turbulence in the jet exhaust. This is most probably not true.

However, it is true that some spectrum does represent this turbulence, and while the assumed spectrum is probably not correct, it is felt that in the absence of any better description, the Kolmogorov spectrum is satisfactory. This question will be investigated in future work.

2. ABSORPTION

Absorption of the 10.6μ CO_2 laser beam in the jet exhaust could be due to many species; candidate molecules include water, carbon dioxide, carbon monoxide and ethylene $\left(C_2H_4\right)$.

Water vapor absorbs broad band in the IR. However, because of the high temperatures and because no water injection was employed on this engine, its effect is considered negligible. Carbon monoxide has a strong absorption band centered at 4.7μ. Though it is present in copious amounts, it should produce little absorption in the 10μ region. Ethylene nearly absorbs CO_2 radiation resonantly, having a band centered at 10.52μ. Even a trace of ethylene present in the exhaust could produce substantial beam degradation. The actual amount present will be the subject of later study.

Carbon dioxide can absorb 10.6μ radiation resonantly if the absorbing molecule is in the (100) vibrational state. This level is about 0.17 ev above the ground state and so its population exhibits a fairly strong temperature dependence. Extrapolation of recent measurements indicates 4.5 torr of CO_2 in an otherwise standard atmosphere has an effective absorption coefficient of about 0.003 m^{-1} (Ref. 8). The exhaust environment had an average thermal temperature of about 500° K. Assuming thermal equilibrium and neglecting thermal enhancement of collision broadening, the Boltzmann population of CO_2 molecules in the 0.17 ev (100) vibrational state should be about an order of magnitude above that at room temperature. The corresponding increase in the expected absorption coefficient to 0.03 m^{-1} is well within our observations.

3. SCINTILLATION

The scintillation measurements of the 10.6μ beam are statistical in nature and most probably some of the higher frequency components were filtered out because of the slow response of the detector. Inclusion of these high frequency scintillations would lead to an increase in the variance and a subsequent increase in the structure constant. In the scintillation measurements, it was assumed that the receiving aperture (4 mm) was small compared with the actual beam diameter ($\simeq$4 inches) so that the beam approximates a plane wave.

4. BEAM SPREAD

The results for beam spreading given in tables V through VII follow a logical pattern. For propagation paths further behind the jet exhaust the beam encounters less turbulence and, consequently, less beam spread. Higher engine power settings led to greater degrees of turbulence as evidenced by the values of C_n. The difference in C_n for 90 and 100 percent engine power is relatively small. Referring to table I, however, it is evident that the difference in fuel flow rate and engine temperature between 90 and 100 percent is small and consequently one would expect the difference in the beam spread to be small.

The three methods of data analysis used here produce results for C_n which agree for corresponding collimated and focused beams to within a factor of two. Other methods, however, may not yield such close agreement. We do not attempt here to indicate which method is more correct. Subsequent work may clarify this situation.

The results given in tables V through VII show a structure constant that is two orders of magnitude larger than the structure constant normally taken as characteristic of strong atmospheric turbulence $\left(C_n = 5 \times 10^{-7} m^{-1/3}\right)$(Ref. 2).

SECTION V

FUTURE STUDIES

Future studies should concentrate on the following areas.

(1) Mapping the turbulence in the jet exhaust using the laser as a probe;

(2) Further investigation of scintillation using high-speed detectors and recorders;

(3) Determining the effect of focusing in different planes in order to determine the condition which gives maximum intensity in a different receiving plane.

APPENDIX I

BEAM SPREADING OF CO_2

Attempts to measure beam spreading of the 10.6μ beam provided little success. As discussed previously, the highly multimode nature of the CO_2 laser and the inherent operating instabilities made accurate measurements difficult. The results from two of these attempts are presented here.

On 11 and 12 February, the CO_2 beam was propagated along the path indicated in figure 1. The beam diameter in the receiver plane under quiescent conditions was approximately 75 mm. Power readings were taken with a variable aperture calibrated in steps of 25 mm and the results are indicated in figure 8. Spreading of the CO_2 beam is not readily apparent from the figure.

On 17 February, the CO_2 laser was operated with a telescope consisting of two germanium lenses. A very poor focus was obtained in the receiver plane of approximately 1 inch in diameter under quiescent conditions. Power readings were taken using a variable aperture calibrated in steps of 2 mm and the results are shown in figure 9 for the jet engine at idle.

The theoretical spreading for the CO_2 beam can be calculated using the structure constant results for the He-Ne propagation of 12 February. On that day the spreading of the focused He-Ne beam indicated a C_n of 2.8×10^{-5}. The theoretical calculation for the spread of a focused CO_2 beam then yields a value of $\omega_t/\omega \simeq 1.04$. If we consider the CO_2 beam as being collimated and use the results of 17 February for the collimated He-Ne beam $C_n = 9.4 \times 10^{-5}$, the theoretical calculation yields a beam spread ratio of $\omega_t/\omega \simeq 1.035$. Figure 9 indicates an expansion of 1.05 which is very close to these theoretical calculations.

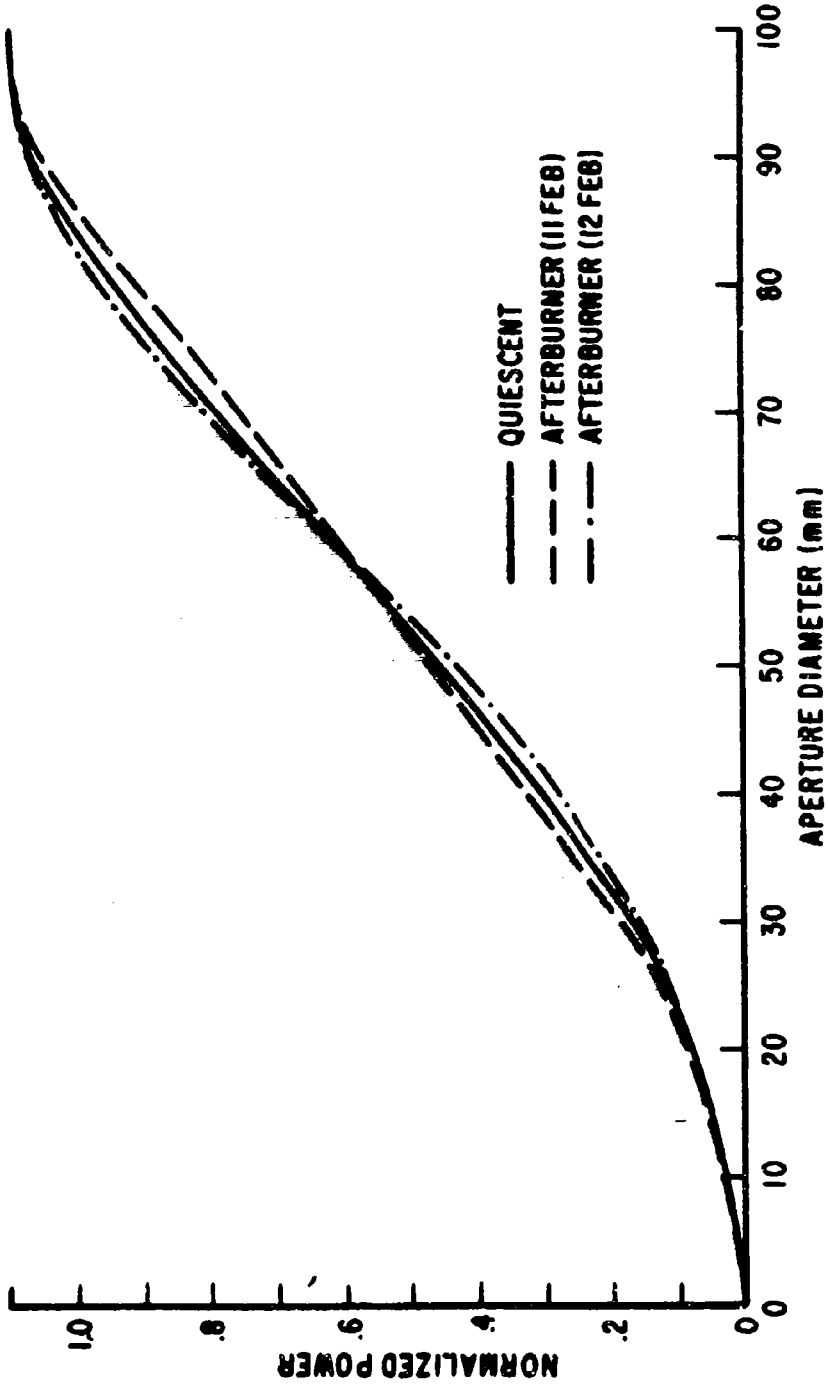

Figure 8. Normalized Power versus Aperture Diameter for Collimated CO_2 Beam on 11 and 12 February 1970

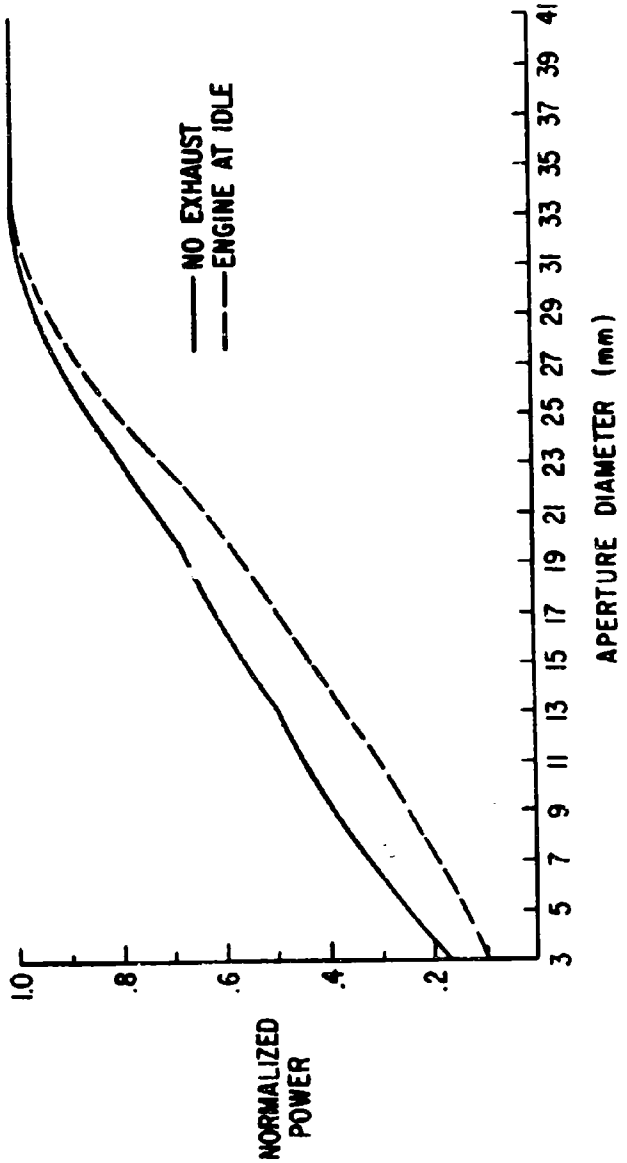

Figure 9. Beam Spread for Focused CO_2 Beam on 17 February 1970

APPENDIX II

NIGHT EXPERIMENT WITH He-Ne

On 2 April 1970, a night experiment was conducted using the He-Ne laser. The laser was situated in the same configuration as on 16 January. The major differences in the path on 2 April were that more of the turbulent exhaust was intercepted (30 meters) and the receiver (a screen) was situated 500 meters away. All measurements were made directly from the screen by the observers and a 35 mm camera.

Without the engine exhaust, the focused beam size was approximately 5 mm. The central spot was well defined and whisper modes from the laser were clearly visible around the central spot. Some fluctuations were observed in the central spot and these fluctuations had a frequency of 10 to 12 cps (the atmospheric wind was about 4 mph). The collimated beam spot size was 1.5 inches in diameter and the same whisper modes and fluctuations across the central spot were observed.

When the engine was turned on (idle), the focused spot very rapidly expanded and soon filled the screen. An estimate of the defocused spot diameter was made at 28 inches (an expansion of approximately 140 times). The defocused spot was very blurred. At 100 percent engine power, the spot size remained approximately the same, and some heat effects from the exhaust were seen to move across the beam.

With the collimated beam, the expansion with the engine at idle was to approximately 15 inches (an expansion of 10 times). The spot was clearly brighter and at 100 percent engine power dark areas were observed in the beam.

When the jet engine was shut down a noticeable vertical structure was observed in both focused and collimated beams. This vertical structure was caused by the heat rising from the concrete slab on which the engine rested. Also apparent was a sputtering of the spot as hot gas moved across the beam path. The photographs for the collimated beam are shown in figures 10 through 15.

NOT REPRODUCIBLE

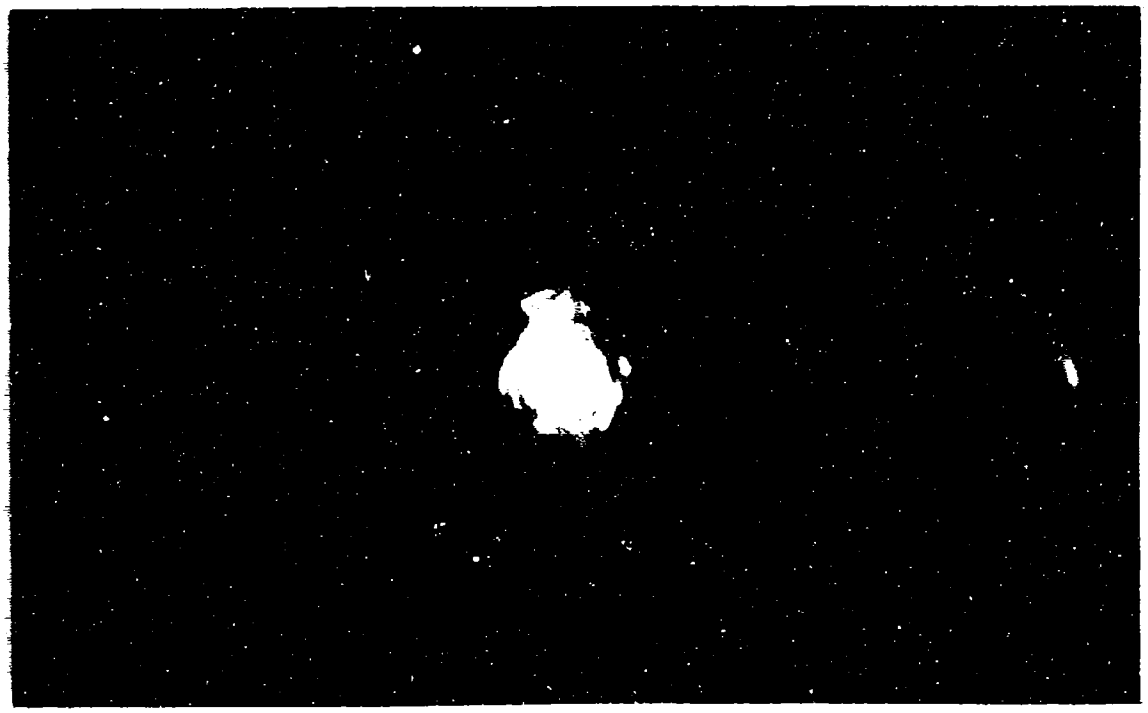

Figure 10. Collimated Beam Before Jet Engine was Started. Note that Whisper Modes are Visible Outside the Main Beam.

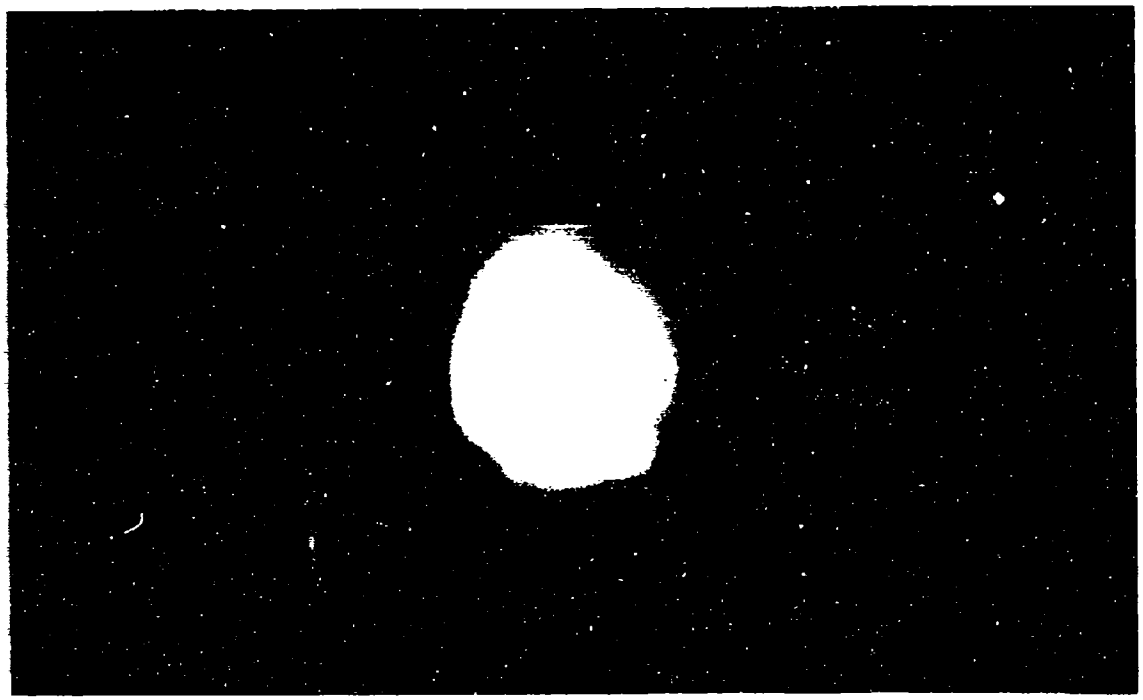

Figure 11. As the Jet Engine is Started, the Beam Immediately Begins to Expand. The Expansion Shown here is not Radially Symmetrical.

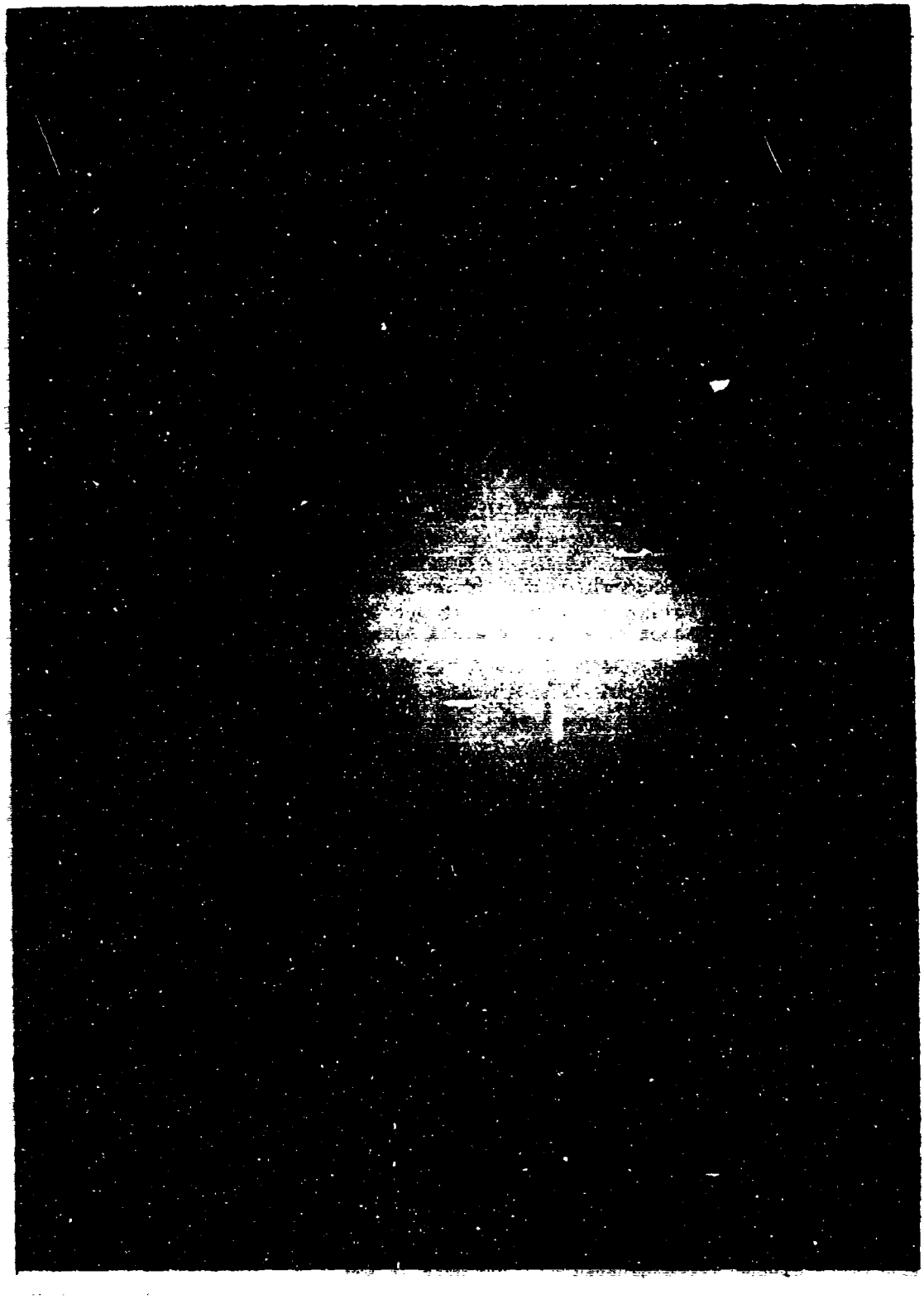

Figure 12. Expanse of the Collimated Beam with the Jet Engine at Idle Power

NOT REPRODUCIBLE

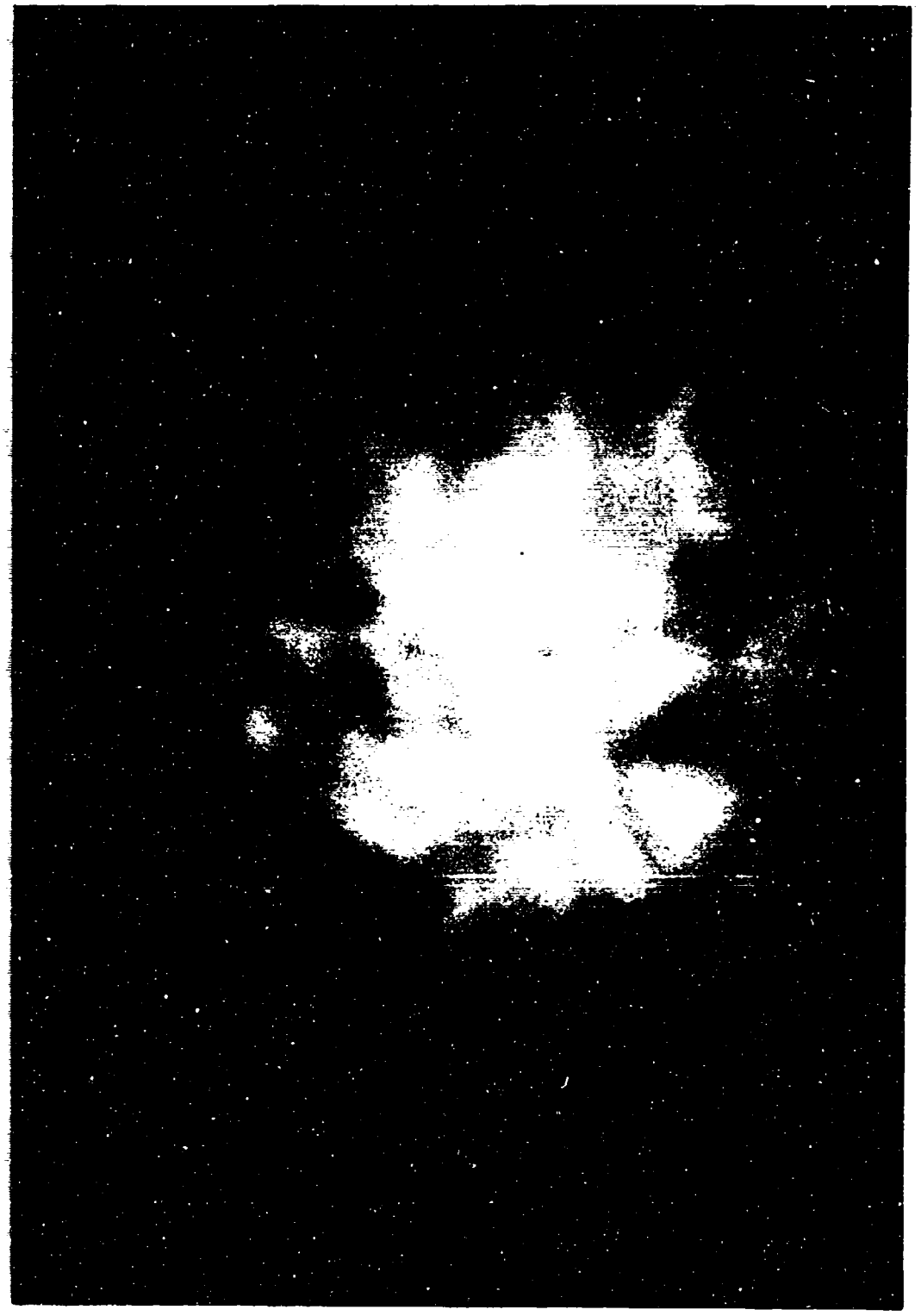

Figure 13. Expanded Beams with the Jet Engine in Afterburner. The Dark Spots Throughout the Expanded Beam were Observed to Move Horizontally Left to Right Through the Beam. The Laser was Located on the Left Side of the Exhaust with the Receiving Screen on the Right.

NOT REPRODUCIBLE

NOT REPRODUCIBLE

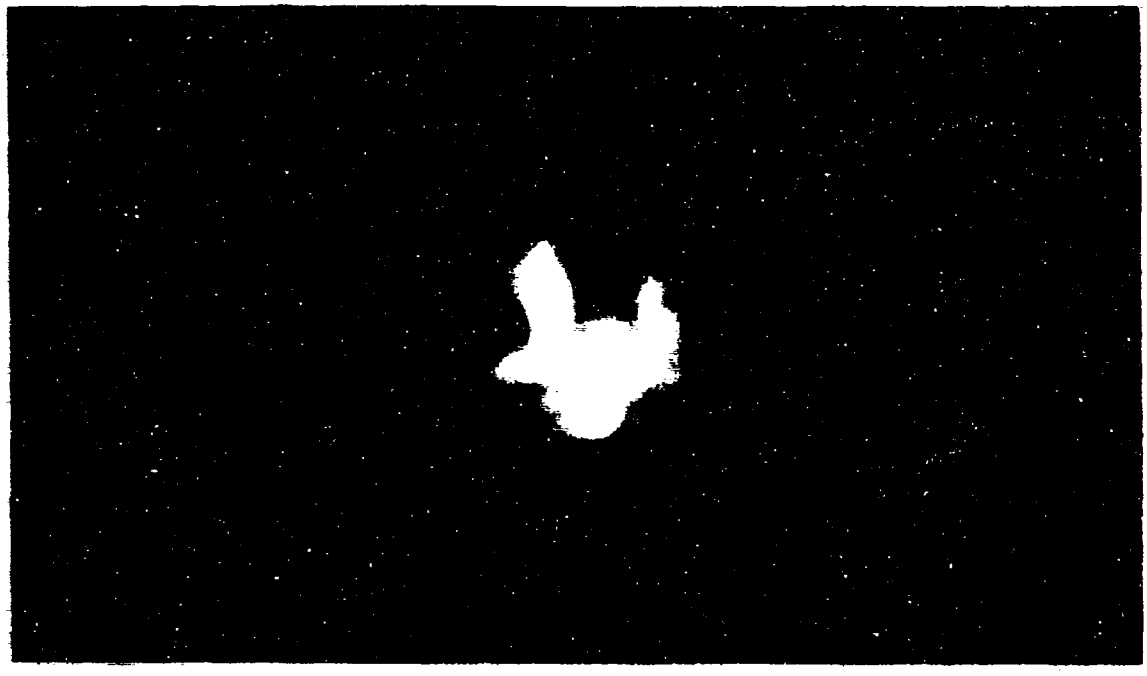

Figure 14. Sputtering of the Beam After Jet Engine Shut-Down. Note the Vertical Structure of the Sputtering Caused by the Rising Hot Gases Immediately Behind the Jet Engine.

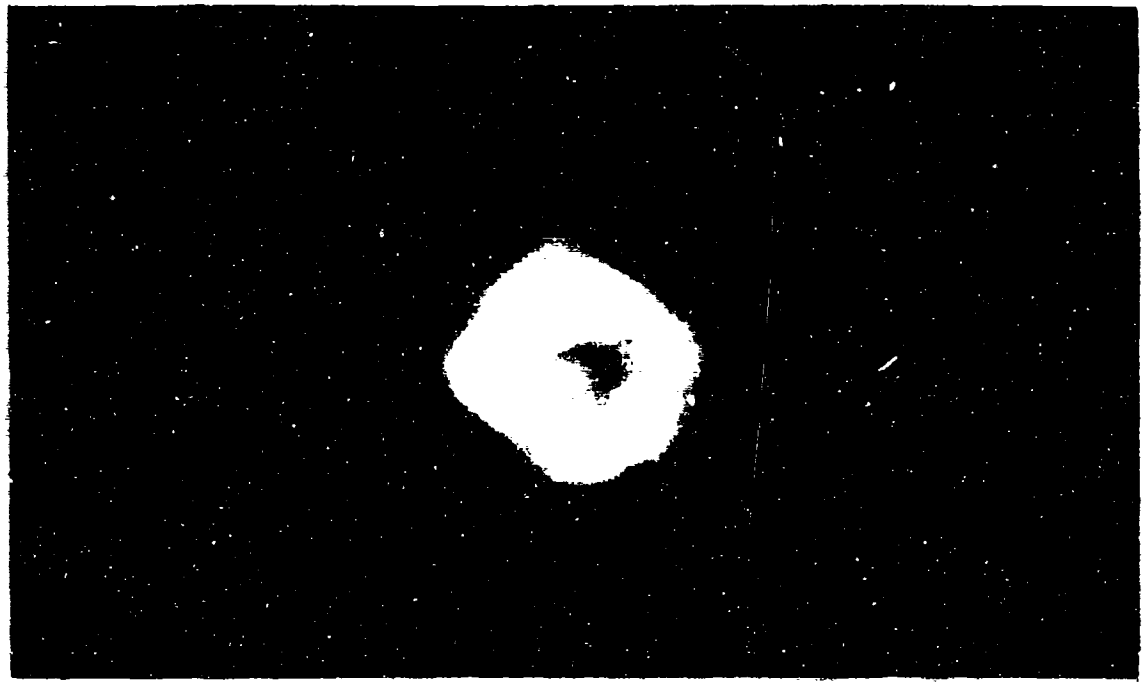

Figure 15. Another Form of Sputtering Observed After Engine Shut-Down-- This One with What Seems to be a Ring Shape.

REFERENCES

1. Tatarski, V. I., Wave Propagation in a Turbulent Medium, McGraw Hill, New York, 1961.

2. Davis, J. I., "Consideration of Atmospheric Turbulence in Laser Systems Design," presented at the Conference on Atmospheric Limitation to Optical Propagation, Boulder, Colorado, 17 March 1965.

3. Fried, D. L., and Seidman, J. B., "Laser-Beam Scintillation in the Atmosphere,: Jour Opt Soc of Am, 57, 2, p. 181, 1967.

4. Gebhart, F. G., The Log-Amplitude Mean Valve for Laser Beam Propagation in the Atmosphere, with Applications for Optical Communications, The Ohio State Univ Electro Science Laboratory, TR 2156-8, 16 May 1968.

5. Wright, N. J. and Schultz, R. J., "Measurement of the Refractive Index Structure Coefficient - C_n," BRL Memorandum Report 1885, December 1967.

6. Bennett, Charles, Air Force Weapons Laboratory, Kirtland AFB, NM, Personal Communication.

7. Ishimaru, A., "Fluctuations of a Focused Beam Wave for Atmospheric Turbulence Probing," Proc IEEE, 57, p. 407, 4 April 1969.

8. Gullberg, K. et al., "Absorption Measurements in Gases with CO_2 Laser Radiation," Arkiv for Fysik, Bd 37, nr 23, p. 362, 1968.

UNCLASSIFIED
Security Classification

DOCUMENT CONTROL DATA - R & D

(Security classification of title, body of abstract and indexing annotation must be entered when the overall report is classified)

1. ORIGINATING ACTIVITY (Corporate author)
Air Force Weapons Laboratory (LRO)
Kirtland Air Force Base, New Mexico 87117

2a. REPORT SECURITY CLASSIFICATION
UNCLASSIFIED

2b. GROUP

3. REPORT TITLE
LASER BEAM PROPAGATION THROUGH JET EXHAUSTS

4. DESCRIPTIVE NOTES (Type of report and inclusive dates)
January 1970 through April 1970

5. AUTHOR(S) (First name, middle initial, last name)
Keith G. Gilbert, Capt, USAF; Charles B. Hogge, Capt, USAF; Walter L. Visinsky, Capt, USAF

6. REPORT DATE
December 1970

7a. TOTAL NO. OF PAGES
44

7b. NO. OF REFS
8

8a. CONTRACT OR GRANT NO.

b. PROJECT NO. 644A

c. Task 2

d.

9a. ORIGINATOR'S REPORT NUMBER(S)
AFWL-TR-70-128

9b. OTHER REPORT NO(S) (Any other numbers that may be assigned this report)

10. DISTRIBUTION STATEMENT This document is subject to special export controls and each transmittal to foreign governments or foreign nationals may be made only with prior approval of AFWL (LRO), Kirtland AFB, NM. Distribution is limited because of the technology discussed in the report.

11. SUPPLEMENTARY NOTES

12. SPONSORING MILITARY ACTIVITY
AFWL (LRO)
Kirtland AFB, NM 87117

13. ABSTRACT

(Distribution Limitation Statement No. 2)

CO_2 (10.6 micron) and He-Ne (6328Å) laser beams were passed through the highly turbulent region in the exhaust of a jet engine (J-57 with afterburner). Experimental information was obtained on the absorption, scattering and turbulence effects of the jet exhaust on both laser beams for various propagation paths. Estimates of a structure constant that would characterize the turbulence in the exhaust are made from the beam spread of focused and collimated beams. The structure constant obtained in this manner is then compared with the structure constant determined from scintillation measurements on the CO_2 beam and with the results of hot-wire anemometer readings in the exhaust. The various methods yield results for the structure constant that are in good agreement. (typically a structure constant of the order of $3 \times 10^{-5} m^{-1/3}$).

DD FORM 1 NOV 65 1473

UNCLASSIFIED
Security Classification

UNCLASSIFIED
Security Classification

14. KEY WORDS	LINK A ROLE	LINK A WT	LINK B ROLE	LINK B WT	LINK C ROLE	LINK C WT
Lasers						
Jet exhaust						
Propagation						
Turbulence effects						
Scintillation						
Absorption						
Beam spread						

UNCLASSIFIED
Security Classification